Calcium carbonate based phosphogypsum: A sustainable solution for thermochemical energy storage

Saad Rmail[1*], *Ayoub* El Karch[1], *Hmida* Slimani[1], *Abdechafik* El Harrak[1], *Abdeslam* El Bouari[1,2], *Hanane* Ait Ousaleh[1], *Abdessamad* Faik[1]

[1]College of Chemical Sciences and Engineering (CCSE), Laboratory of Inorganic Materials for Sustainable Energy Technologies (LIMSET), University Mohammed VI Polytechnic (UM6P), Benguerir, 43150, Morocco

[2]Laboratory of Physical Chemistry of Applied Materials (LCPMA), Chemistry Department, Hassan II University of Casablanca, Faculty of Science Ben M'sik, Bd Commandant Driss Al Harti, Casablanca 20670

Abstract. The large number of stockpiles of phosphogypsum (PG), an abundant by-product during the process of producing phosphoric acid, is accompanied by many challenges owing to the toxicity of certain substances contained within PG. In this work, we investigate the transformation of PG into calcium carbonate ($CaCO_3$) as an appropriate thermochemical energy storage (TCES) agent using the reversible reaction $CaCO_3 \leftrightarrow CaO+CO_2$. For the transformation of PG into $CaCO_{3(1)}$ and $CaCO_{3(2)}$, PG was reacted with Na_2CO_3 and K_2CO_3 in a proper aqueous medium, respectively. The composition and crystal structures of the resulting products have been confirmed by XRF and XRD to be highly pure (> 97%) with about 2% SiO_2 in situ in $CaCO_3$ obtained from PG. SEM-EDS analysis demonstrates that rhombohedra with homogeneous element distribution have been obtained successfully. STA tests in the temperature range from 550-800 °C within 10 decarbonation and carbonation cycles demonstrate the stability and reversibility of CO_2 capture and release for both types of $CaCO_3$ with $CaCO_{3(1)}$ having higher retention (>23% after 10 cycles) compared to $CaCO_{3(2)}$ (~19%). The above results confirm that $CaCO_3$ obtained from PG, especially $CaCO_{3(1)}$, is a suitable choice for TCES.

Keywords: Solid-Gas Reaction; Metal Carbonate; Thermochemical Energy Storage; Heat Energy Storage; Phosphogypsum Valorization; Waste Valorization

*Corresponding author: saad.rmail@um6p.ma

1. Introduction

The development of new energy sources with a durable lifespan has now become evident in light of the increasing need for the storage of heat energy, especially in locations where the sole heat source is solar energy and there is a dire need to adopt sustainable methods of energy production [1]. The increasing global need to ensure zero CO_2 emissions has made it all the more imperative to seek new ways of generating sustainable energy. In this study, we will attempt to see how phosphogypsum (PG) can be converted to calcium carbonate ($CaCO_3$). By making use of the PG in converting it to $CaCO_3$, not only do we resolve waste management issues but also create useful energy resources [2][3]. Phosphogypsum is commonly produced during the wet process of phosphoric acid production from concentrate phosphate rock and may create environmental problems because of its hazards, huge stockpile sizes, and high maintenance cost [4–6]. In order to minimize the footprint of huge amounts of PG, this paper shows proof of concept that the potential of PG as an inexpensive technology to store heat energy is highly promising as TCM product. The conversion of phosphogypsum (PG) into calcium carbonate ($CaCO_3$) for thermochemical energy storage (TCES) has attracted considerable interest [7]. One of the main issues associated with the above processes is the safe storage of heat. Reactions involving carbon dioxide at high temperatures fall under another important type of thermochemical processes, creating concern about the environment and requiring effective technologies of gas storage. Valorization and fabrication of calcium carbonate ($CaCO_3$) from phosphogypsum (PG) using the solar driven process constitute a sustainable and innovative process of using renewable energy and treating industrial waste. The use of solar energy in the solar heater (calciner) for the thermal dissociation of $CaCO_3$ into CaO and CO_2. The CaO formed as such is stored in a separate storage, while the CO_2 is captured and stored in an industrial CO_2 storage device. The next step involves the reaction between the stored CaO with the captured CO_2 in a carbonator to form calcium carbonate ($CaCO_3$) that can be used for various purposes [8]. The general reaction for $CaCO_3$ can be written as follows: $CaCO_{3(solid)} + 177.8\,kJ/mol \leftrightharpoons CaO_{(solid)} + CO_{2\,(gas)}$ (1)

This cyclic process suggests an energy storage method that offers a chance to use CO_2 and therefore reduces the carbon footprint. The inclusion of a CO_2 industrial gas turbine improves the system's efficiency by possibly producing extra power from the stored CO_2, which is accomplished by harnessing solar energy for the chemical processes [9]. Moreover, this technique tackles the environmental issues linked to the disposal of phosphogypsum, aiding in the development of a circular economy and the sustainable progression of industrial practices.

2. Materials and Methods

2.1 Materials and Synthesis

Phosphogypsum was sourced from OCP Jorf Lasfar facility (Morocco). Sodium carbonate (Na_2CO_3, ≥99.5%, Sigma-Aldrich) and potassium carbonate (K_2CO_3, ≥99.5%, Sigma-Aldrich) were used as chemical precursors at a molar ratio of $[SO_4]^{2-}/[CO_3]^{2-} = 1$.

2.1.1 Synthesis procedure

10 g of pre-ground PG was dissolved in 150 mL distilled water at 75°C for 30 minutes. Either 6.15 g Na_2CO_3 (yielding $CaCO_{3(1)}$ or 8.027 g K_2CO_3 (yielding $CaCO_{3(2)}$ was added to the respective beakers and subjected to magnetic stirring at 75°C for 3 hours. The resulting solid precipitate was filtered, rinsed with distilled water several times to eliminate any leftover carbonate precursors, and dried overnight at 100°C. This synthesis method takes advantage of the varying solubility between calcium sulfate and calcium carbonate in an aqueous solution at moderate temperatures. The theoretical mass calculations were derived from the

stoichiometric conversion of calcium sulfate dihydrate ($CaSO_4.2H_2O$), which is found in raw phosphogypsum, to calcium carbonate ($CaCO_3$).

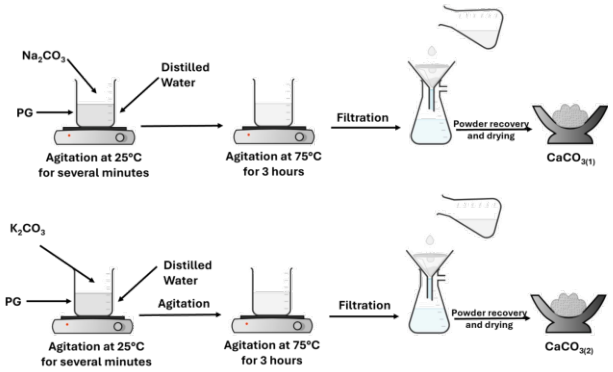

Fig 1. Synthesis process used to prepare $CaCO_{3(1)}$ and $CaCO_{3(2)}$ from Phosphogypsum (PG), Na_2CO_3 and K_2CO_3.

2.1.2 Synthesis Mechanism

The reaction proceeds through an aqueous metathesis pathway wherein sulfate ions are displaced by carbonate ions:

$$CaSO_4.2H_2O + Na_2CO_3 \rightarrow CaCO_3\downarrow + Na_2SO_4 + 2H_2O \quad (2)$$

$$CaSO_4.2H_2O + K_2CO_3 \rightarrow CaCO_3\downarrow + K_2SO_4 + 2H_2O \quad (3)$$

The reason why this reaction takes place is the low solubility product constant of calcium carbonate ($K_{sp} \approx 3.36 \times 10^{-9}$) relative to that of calcium sulfate dihydrate ($K_{sp} \approx 2.4 \times 10\text{-}5$), which makes the formation of $CaCO_3$ more favorable [7]. The temperature of 75 °C and time period of 3 hours were chosen based on the optimization of calcium content conversion and low energy requirement. The temperature selected is enough to increase the rate of reaction without causing any change in crystal structure of $CaCO_3$ (aragonite/vaterite phases) [10].

2.2 Characterization Techniques

Technique	Instrument	Conditions
XRF	Rigaku X-ray Fluorescence	Qualitative and semi-quantitative elemental analysis
XRD	Anton Paar Dynamic 500	2θ = 5-85°, step = 0.02°; Rietveld refinement via FullProf
SEM-EDS	TESCAN TIMA	Carbon coating; elemental mapping and morphology assessment
STA	NETZSCH Jupiter STA 449 F3	10 cycles, 550-800°C, N_2 + CO_2 reactive gas

3. Results and Discussion

Elemental composition analysis on the samples has been done through the Rigaku X-ray Fluorescence (XRF) spectrometer. Qualitative and semi qualitative analysis of the chemical

composition is undertaken in order to ensure a better understanding of the elements present in the PG, as well as the Calcium carbonates produced using PG.

Elemental composition analysis brings some essential points that are vital to the evaluation of the success of the synthesis and changes of the composition. The first phosphogypsum has CaO content of 32.32%, being slightly lower than previous results from similar OCP Jorf Lasfar samples (usually between 35% and 37%). This might be due to differences in phosphate ores used or synthesis conditions. Large P-Feu content of 20.40%, which stands for loss on ignition and shows presence of organic matter and water content in it, proves that the starting PG is indeed hydrated PG ($CaSO_4.2H_2O$). As a result of transformation to calcium carbonate, CaO content increased to 48.10% in $CaCO_{3(1)}$ and 48.30% in $CaCO_{3(2)}$, constituting 49% enrichment. This degree of enrichment is justified according to theoretical considerations based on differences in molar masses for calcium sulfate dihydrate (172.17 g/mol in terms of CaO) and calcium carbonate (100.09 g/mol).

The simultaneous decline in P-Feu content from 20.40% to ~2.8% implies successful elimination of excess water and decomposition of organic compounds in the synthesis and dehydration processes. The reduction in SO3 content from 40.20% (raw PG) to 0.45-0.55% (synthesized carbonates) demonstrates nearly complete conversion of the former to carbonate ions; the possible locations of the residue may be grain boundaries or sulfate phases occurring in trace amounts. The difference in CO_2 content for the two $CaCO_3$ samples (43.82% and 43.31%) is negligibly small (~0.5% and within the acceptable error limits).

Table 1. XRF results for PG, calcium carbonate from sodium carbonate PG source, and potassium carbonate by PG source

a) Quantitative Analysis

Chemical Composition in %	CaO	SiO_2	Al_2O_3	Fe_2O_3	MgO	K_2O	Na_2O	TiO_2	P_2O_5	MnO	P-Feu	Total
PG Raw	32.32	1.80	0.13	0.04	0.09	0.05	0.28	< 0,01	1.11	< 0,01	20.40	56.21
$CaCO_3$/PG/Na_2CO_3 Source ($CaCO_{3(1)}$)	48.10	2.35	0.12	0.05	0.05	0.02	0.47	< 0,01	0.59	< 0,01	2.81	56.56
$CaCO_3$/PG/K_2CO_3 Source ($CaCO_{3(2)}$)	48.30	2.23	0.13	0.07	0.09	0.59	0.13	< 0,01	0.64	< 0,01	2.80	56.98

b) Semi-quantitative Analysis

Chemical Composition in %	CaF_2	SO_3	CO_2	Total. Final
PG Raw	0.97	40.20	97.39	0.97
$CaCO_3$/PG/Na_2CO_3 Source ($CaCO_{3(1)}$)	< 0,01	0.45	43.82	98.83
$CaCO_3$/PG/K_2CO_3 Source ($CaCO_{3(2)}$)	< 0,01	0.55	43.31	98.86

The minor impurities such as Al_2O_3 and Fe_2O_3 have been found to be identical for both raw and synthesized materials, which implies that these impurities must be present in the matrix of the synthesized product in dispersed form or in trace amounts in the calcite matrix. The increase in the amount of K_2O in $CaCO_{3(2)}$ (0.59%) compared to the raw PG (0.05%) shows

that there is some presence of potassium from K_2CO_3 in the washing process, even after repeated washings. This causes excess potassium to be incorporated into the $CaCO_3$ matrix either by electrostatic adsorption or lattice substitution.

The crystal structures of the synthesized compounds are precisely determined using XRD analysis along with Rietveld refinement. Both $CaCO_{3(1)}$ and $CaCO_{3(2)}$ exhibit the trigonal phase of calcite (space group R-3c, hexagonal system) that constitutes the thermodynamically stable phase of $CaCO_3$. The crystallographic data of both samples matches those of pure calcite crystals (a= 4.9896 Å, c = 17.0600 Å) from the literature, confirming the formation of $CaCO_3$ with no polymorphic impurities like aragonite or vaterite [10].

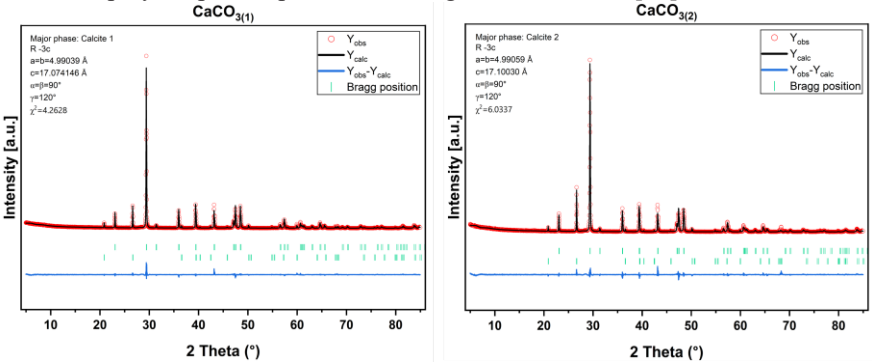

Fig 2. XRD refinement of calcites $CaCO_3$ PG Based.

A good match between the experimental and simulated diffraction patterns is confirmed by low goodness of fit χ^2 values (χ^2 = 5.35 for $CaCO_{3(1)}$ and 6.03 for $CaCO_{3(2)}$) and low weighted R-factors (R_{wp} = 11.1% and 12.4%, correspondingly), indicating successful refinement and reliable phase quantification. Minor quartz phase (SiO_2) detected in both samples (2.07% and 2.09%, respectively) is explained by the presence of residual silicon dioxide, being a product of the raw phosphogypsum. Presence of such crystalline phase, resulting in in-situ silicon dioxide doping of the samples, may improve thermal stability of the materials under investigation and be considered as "natural doping," which has already been proven to be effective in similar calcium carbonate samples [11]. As can be seen, quartz has a hexagonal structure of wurtzite type (α-quartz) rather than monoclinic high-temperature β-quartz [12].

Table 2. Rietveld refinement of calcium carbonate (calcite) synthesized from Phosphogypsum

Main Phases		a (Å)	b (Å)	c (Å)	α	β	δ	R_p, R_{wp}, R_{exp}	Chi 2	Fraction (%)
Calcite 1	$CaCO_{3(1)}$	4.99039	4.99039	17.07421	90°	90°	8.31	8.31, 11.1, 2.78	5.35	97.93
	$SiO_{2(1)}$	4.91456	4.91456	5.40672	90°	90°	120°			2.07
Calcite 2	$CaCO_{3(2)}$	4.99059	4.99059	17.10030	90°	90°	8.84	8.84, 12.4, 2.04	6.03	97.91
	$SiO_{2(2)}$	4.91411	4.91411	5.49518	90°	90°	120°			2.09

This remarkable similarity of lattice parameters in both $CaCO_{3(1)}$ and $CaCO_{3(2)}$, even when different alkali metals were used in the synthesis of $CaCO_3$, clearly shows that the alkali metals do not participate in formation of the crystal lattice. Only small deviations of the parameters of the c axis can be seen (17.07421Å compared to 17.10030Å, hence $\Delta c \approx 0.026$ Å), but these deviations can be explained by experimental error. It is important for this particular observation because it proves that the purity of the obtained phase was preserved during the alkali substitution process.

The simultaneous thermal analysis (STA) experiments examined the reversibility and stability of the decarbonation/carbonation cycles over 10 successive runs at temperatures ranging from 550°C to 800°C. The cycling procedure used conditions pertinent to concentrating solar power (CSP) integration:

- Heating rate: 10°C/min in a nitrogen atmosphere until reaching 800°C
- Isothermal hold: 20 minutes maintained at 800°C
- Carbonation/cooling: Increase temperature to 550°C at 10°C/min in a carbon dioxide atmosphere
- Isothermal hold: 15 minutes sustained at 550°C

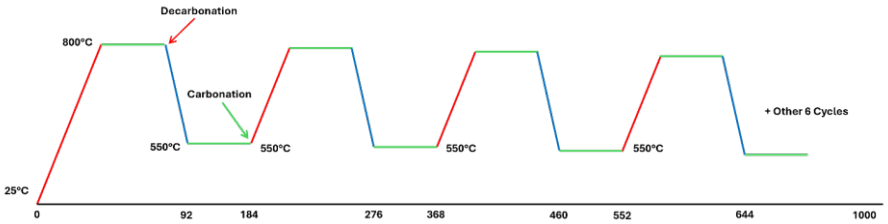

Fig 3. Schematic of the Decarbonation/Carbonation cycling conditions for the developed materials using STA.

$CaCO_{3(1)}$ cycling behavior: This material shows a steady decrease in weight throughout all 10 cycles, with the initial cycle exhibiting the largest weight loss (~35-40%) as a result of the decomposition of $CaCO_3$ into CaO and CO_2. In subsequent cycles, the weight loss stabilizes at around ~30-32%, indicating the loss of easily absorbed water and CO_2 during the first cycle, followed by reaching a steady state. The lack of any shift in peak positions across the cycles indicates thermal stability and that no phase transformations occur during cycling.

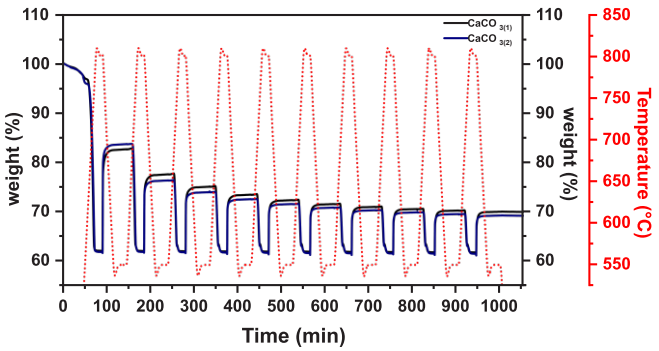

Fig 4. Simultaneous thermal analysis (STA) results of 10 cycles of Calcites derived from Phosphogypsum sources.

$CaCO_{3(2)}$ cycling behavior: This sample shows a slightly greater weight loss in the initial cycle (~38-42%) but stabilizes at ~28-30% in subsequent cycles, which is somewhat lower than the results from $CaCO_{3(1)}$. Comparison and Interpretation: The better results observed from $CaCO_{3(1)}$ (greater stable-state mass losses that indicate higher reversibility in CO_2 cycles) are related to improved phase purity and surface features that favor decarburization and carburization reactions. The slight but appreciable difference in mass losses (around 2%) from $CaCO_{3(1)}$ relative to $CaCO_{3(2)}$ provides a useful improvement for thermochemical energy storage due to enhanced CO_2 conversion and cycling reversibility. Considering the $CaCO_3$/CaO reaction enthalpy, the measured energy density can reach ~1952 kJ/kg [13].

3.2 Thermal conversion(X) of charge curves of $CaCO_{3(1)}$ and $CaCO_{3(2)}$.

Fig 5 illustrates the thermal conversion cycles (X) for calcium carbonate specimens ($CaCO_{3(1)}$ and $CaCO_{3(2)}$) exceeding 10 cycles of carbonation process. The presented conversion curves reflect the ability of the material to capture and release the CO_2 during many cyclic conversions, which is an important characteristic of thermochemical energy storages. The conversion, defined as a share of the amount of CO_2 captured by material from calcium carbonate, reaches about 70% in both samples in each 20 minutes cycle time period. The conversion level reflects that the chemical conversion is approaching its completion, highlighting good performance of the materials under study

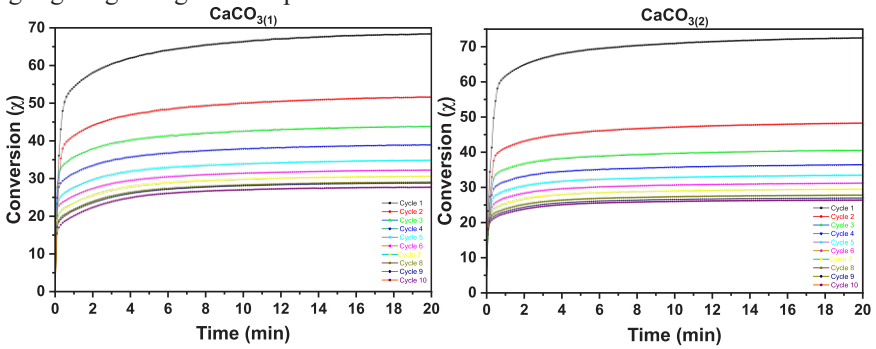

Fig 5. Thermal conversion (X) of $CaCO3_{(1)}$ and $CaCO_{3(2)}$ over 10 cycles.

i) $CaCO_{3(1)}$ Conversion Cycle Graph: The initial conversion attained is close to 70% within the first 15-20 minutes of cycle one at 800°C. It is important to note that the conversion attained is still 23% at the end of cycle 10. Therefore, the conversion attained at this point is 23% of the total maximum possible conversion. This implies that the extent of the remaining decarbonation reaction is around 33% of the total decomposed amount.

ii) $CaCO_{3(2)}$ conversion profile: Although the conversion at the start is nearly 68-70% (the same as $CaCO_{3(1)}$), it shows a lower end-point conversion (approximately 19% at cycle 10), equivalent to 27% of the first-cycle conversion value. Due to the faster drop in conversion efficiency compared to $CaCO_{3(1)}$, this suggests either faster sintering with reducing of the surface area for reaction or the formation of kinetic barriers at the oxidized surface layer.

The difference in their cycling behavior can be attributed to improved thermal cycling stability of the $CaCO_3$ produced from sodium carbonate because of better surface chemistry, as well as less tendency to undergo unfavorable phase transformations at elevated temperatures [9].

3.3. SEM results

3.3.1. SEM results of PG raw

The morphological appearance of raw phosphogypsum clearly suggests the presence of $CaSO_4.2H_2O$ in the dihydrate phase. SEM investigation reveals monoclinic crystal forms in the shape of needles/laths, ranging in size from 100 nm to a few microns. It is well established that phosphogypsum exhibits characteristic tubular/prismatic morphology due to preferred crystallographic growth along the direction during the formation reaction in sulfuric acid leaching. Raw phosphogypsum particles are moderately rough and reveal obvious surface impurities and agglomeration, suggesting precipitation occurring at an industrial level.

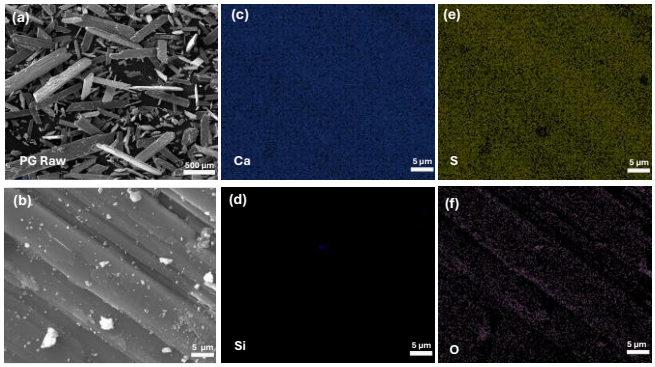

Fig 6. Morphology and elemental mapping images of phosphogypsum (PG) Raw bought from JORF LASFAR.

EDS elemental mapping confirms the presence of calcium (Ca) in all particles in equal distribution, indicative of the stoichiometric ratio of $CaSO_4$. Elemental mapping for S indicates a similar trend to Ca, thus validating the association of S with sulfate. The distribution of oxygen (O) follows a similar trend to Ca and S, as expected within the structure of sulfate. However, the most important aspect of elemental mapping is the identification of silicon (Si), which shows localized contamination restricted to the particle surfaces and grain boundaries. This indicates that Si contaminants (presumably from silicates in phosphate ores) are not uniformly dispersed but act as surface contamination [14].

3.3.2. SEM results of $CaCO_{3(1)}$ and $CaCO_{3(2)}$ before cycling.

$CaCO_{3(1)}$, which was synthesized using sodium carbonate, displays high-magnification SEM images of well-defined rhombohedral crystals with typical dimensions of 5 to 30 micrometers. These crystals have smooth surfaces with very few surface flaws, thus suggesting that the precipitation process was well-controlled with negligible surface roughness. From elemental analysis, it is apparent that the calcium and carbon elements are uniformly distributed on the crystal, with trace amounts of silicon present. This uniform distribution and the well-defined crystals suggest that the process of precipitation occurred through homogeneous nucleation.

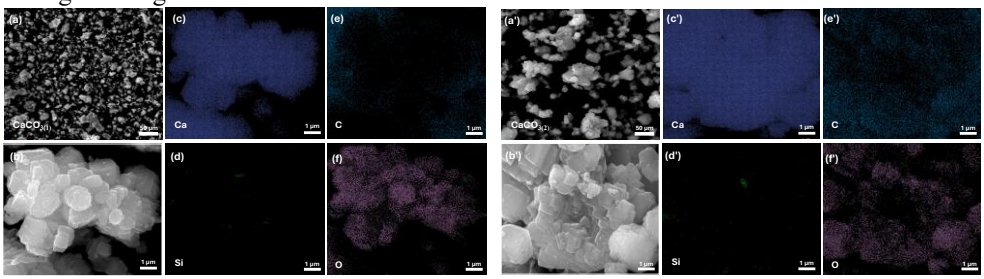

Fig 7. Morphology and elemental mapping images of $CaCO_{3(1)}$ and $CaCO_{3(2)}$ rhombohedral calcites before cycling.

$CaCO_{3(2)}$, obtained from potassium carbonate, exhibits a morphological structure akin to $CaCO_{3(1)}$ but displays certain morphological variations. The crystal facets display some roughness, and surface irregularities are evident, suggesting that the precipitation process was relatively faster. EDS mapping reveals the elemental composition of calcium and carbon, but the emission intensity of potassium is considerably stronger around the grain boundaries and surface regions compared to the bulk regions of the crystal, which suggests that potassium ion uptake predominantly occurs via surface or grain boundary interactions.

The systematic analysis revealed that $CaCO_{3(1)}$ possesses superior crystallinity, with distinct facets and minimal surface defects. It is suitable for thermal cycling due to its smooth surface,

which reduces nucleation sites for thermal reconstruction and sintering. The presence of a slightly rougher surface on $CaCO_{3(2)}$ is helpful for the diffusion of CO_2 during decarbonation. However, it promotes sintering at elevated temperatures.

3.3 SEM results of $CaCO_{3(1)}$ and $CaCO3_{(2)}$ after cycling.

After cycling, $CaCO_{3(1)}$: There is some degree of surface polishing and incipient sintering in the sample. The previously sharp edges of the crystals are now somewhat rounded (the radius of curvature of the edges being estimated to increase from below 50 nm to about 200-300 nm). Calcium and carbon are uniformly distributed in the material without phase segregation. Notably, the rhombohedral structure of the material is still preserved, implying that the material can withstand several cycles of expansion and contraction without mechanical damage. The sintering process is consistent with thermal surface diffusion at 800°C, a well-known phenomenon for $CaCO_3$/CaO systems.

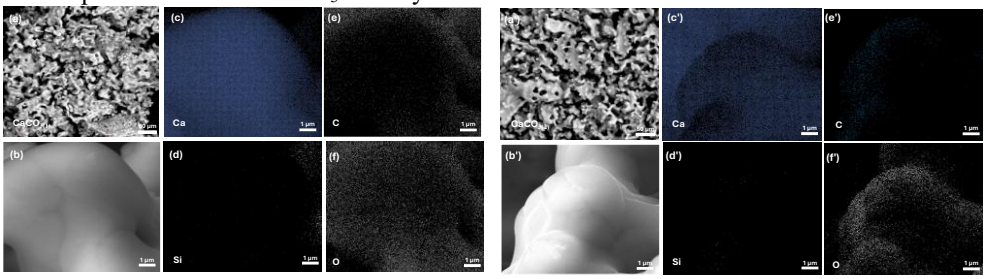

Fig 8. Morphology and elemental mapping images of $CaCO_{3(1)}$ and $CaCO_{3(2)}$ rhombohedral calcite after cycling.

Post-cycling of $CaCO_{3(2)}$: This sample displays a relatively greater increase in surface roughness due to cycling than $CaCO_{3(1)}$. The crystalline surfaces have changed from having a relatively smooth appearance to exhibiting increased textural features, with an increase in defects, which suggests faster surface restructuring or varying sintering mechanisms. The presence of the carbonate phase is confirmed by EDS maps, while the silica concentrated at grain boundaries remains visible after cycling, which may contribute to limiting sintering. Despite these morphological changes, both materials preserve structural integrity and the rhombohedral calcite morphology, indicating that the calcite phase remains stable during CO_2 cycling.

4. Conclusion

This work shows how phosphogypsum can be easily converted into high-purity calcite ($CaCO_3$) by using simple aqueous conversion techniques involving Na_2CO_3 or K_2CO_3 to convert an abundant industrial waste material into a useful thermochemical energy storage compound. The synthesized $CaCO_3$ from PG is found to have stable and repeatable decarbonation and carbonation reactions at appropriate temperatures (550-800 °C) after 10 cycles, suggesting its suitability as a candidate material for use in TCES applications. Structural and elemental analysis reveals that the dominant phase formed is calcite, along with minor in-situ SiO_2. In summary, the $CaCO_{3(1)}$ produced from Na_2CO_3 possesses a relatively better retention of the conversion during cycling compared to its counterpart obtained from the K_2CO_3 route, thus making the sodium-carbonate based approach the preferred choice for scalable value addition in PG via the TCES concept. Further studies need to be undertaken beyond the 10-cycle mark to determine any degradation modes associated with the degradation of the PG-derived $CaCO_3$ in order to assess its long-term performance in TCES applications. In addition, there needs to be an optimization of the process variables such as temperature, solid-to-liquid ratio, and washing techniques to increase conversion efficiencies while preventing any sintering. Systematically, the evaluation of the efficiency, technical and economic challenges of integrating this technology into a lab-scale CSP-TCES

system would enable an analysis of the advantages and disadvantages in comparison with carbonate-based systems and sensible heat storage.

Acknowledgements

The authors would like to sincerely thank OCP group for their financial support of the 'Energy, Science & Technology / NRG' program, under Specific Agreement Number 175
As well as PGStorE - Turning phosphogypsum, a by-product from phosphate industry, into valuable low-cost feedstock for thermochemical energy storage systems.

References

[1] S. Rmail, A. El, H. Haouas, H. Slimani, A. El, S. Sair, A. El, A. Faik, H. Ait, Thermochemical energy storage potential of CaCrO4/ CaCr2O4 : Experimental and first-principles insights, J. Energy Storage 148 (2026) 119982. https://doi.org/10.1016/j.est.2025.119982.

[2] F. Akfas, A. Elghali, A. Aboulaich, M. Munoz, M. Benzaazoua, J.L. Bodinier, Exploring the potential reuse of phosphogypsum: A waste or a resource?, Sci. Total Environ. 908 (2024) 168196. https://doi.org/10.1016/j.scitotenv.2023.168196.

[3] U.S. Department of Energy, Energy Storage Grand Challenge Energy Storage Market Report 2020, 2020. https://www.energy.gov/sites/default/files/2020/12/f81/Energy Storage Market Report 2020_0.pdf.

[4] C. Conkline, Potential uses of phosphogypsum and associated risks, Backgr. Inf. Doc. EPA (1992) 2–92.

[5] M. Taha, S.M.A. Wahab, H.S. Gado, M.H. Taha, O.E. Roshdy, Application of Full Factorial Design to Optimize Phosphogypsum Conversion to Calcium Carbonate Egyptian national project EGY 2011 View project Application of Full Factorial Design to Improve Phosphogypsum Conversion Process to Calcium Carbonate, J. Basic Environ. Sci. 4 (2017) 339–350. https://www.researchgate.net/publication/321293103.

[6] S.M.A. Wahab, H.S. Gado, M.H. Taha, O.E. Roshdy, Application of Full Factorial Design to Improve Phosphogypsum Conversion Process to Calcium Carbonate, 4 (2017) 339–350. http://jbesci.org/volume.php?volume=Vol.4 No.4.

[7] J. Sunku Prasad, P. Muthukumar, F. Desai, D.N. Basu, M.M. Rahman, A critical review of high-temperature reversible thermochemical energy storage systems, Appl. Energy 254 (2019) 113733. https://doi.org/10.1016/j.apenergy.2019.113733.

[8] Y. Ennaciri, M. Bettach, Procedure to convert phosphogypsum waste into valuable products, Mater. Manuf. Process. 33 (2018) 1727–1733. https://doi.org/10.1080/10426914.2018.1476763.

[9] C. Ortiz, J.M. Valverde, R. Chacartegui, L.A. Perez-Maqueda, P. Giménez, The calcium-looping (CaCO3/CaO) process for thermochemical energy storage in concentrating solar power plants, Renew. Sustain. Energy Rev. 113, 109252 (2019).109252.

https://doi.org/10.1016/j.rser.2019.109252.

[10] T. Fujimura, K. Matsui, I. Maruyama, Vibrational and First-Principles Analyses of Aragonite , Calcite , and Vaterite CaCO 3 Prepared from 13 CO 2 Isotope, (2025). https://doi.org/10.1021/acsomega.5c06456.

[11] A.A. Khosa, N. ul H. Shah, H.A.N. Xinyue, N. Husnain, Silica Dopant Effect on the Performance of Calcium Carbonate/Calcium Oxide Based Thermal Energy Storage System, Therm. Sci. 28 (2024) 837–850. https://doi.org/10.2298/TSCI230422165K.

[12] S.M. Antao, Quartz : structural and thermodynamic analyses across the a $ b transition with origin of negative thermal expansion (NTE) in b quartz and calcite research papers, (2016) 249–262. https://doi.org/10.1107/S205252061600233X.

[13] H. Zheng, C. Song, C. Bao, X. Liu, Y. Xuan, Y. Li, Y. Ding, Dark calcium carbonate particles for simultaneous full-spectrum solar thermal conversion and large-capacity thermochemical energy storage, Sol. Energy Mater. Sol. Cells 207 (2020) 110364. https://doi.org/10.1016/j.solmat.2019.110364.

[14] M. Dong, J.S. Li, L. Lang, X. Chen, J. Jin, W. Ma, Recycling thermal modified phosphogypsum in calcium sulfoaluminate cement: Evolution of engineering properties and micro-mechanism, Constr. Build. Mater. 373 (2023) 130823. https://doi.org/10.1016/j.conbuildmat.2023.130823.